Beta decay of the new isotopes ^{52}K, ^{52}Ca, and ^{52}Sc; a test of the shell model far from stability

A. Huck, G. Klotz, A. Knipper, C. Miehé, C. Richard-Serre, and G. Walter
Centre de Recherches Nucléaires, 67037 Strasbourg Cedex, France

A. Poves
Departamento de Fisica Teorica, Universidad Autonoma, Madrid 34, Spain

H. L. Ravn
The Isolde Collaboration, CERN 1211 Geneva 23, Switzerland

G. Marguier
Institut de Physique Nucléaire, Université Lyon 1, 69622 Villeurbanne Cedex, France
(Received 4 September 1984)

The nuclides ^{52}K, ^{52}Ca, and ^{52}Sc have been produced by fragmentation of a uranium target with a 600 MeV proton beam. The subsequent β decays to the daughter nuclei ^{52}Ca, ^{52}Sc, and ^{52}Ti have been studied by neutron and γ spectroscopy on sources obtained from on-line mass separation. β decay energies have been determined by β-γ coincidence spectroscopy. In addition to the short half-life of ^{52}K ($T_{1/2}=110\pm30$ ms), we attributed two different half-lives ($T_{1/2}=4.6\pm0.3$ s and $T_{1/2}=8.2\pm0.2$ s) to ^{52}Ca and ^{52}Sc, respectively. A decay scheme has been established for ^{52}K involving five β branches to delayed neutron emitting states between 6.6 and 10.3 MeV and one β branch to a bound level at $E_x=2.56$ MeV. The ^{52}Ca decay scheme accounts for β branches to four levels at 1.64, 2.75, 3.46, and 4.27 MeV for which the deduced logft values restrict the angular momentum and parity to $J^\pi=1^+$. For the ^{52}Sc ground state, strong β transitions to the 2^+ (1.05 MeV) and the (4^+) (2.32 MeV) levels in ^{52}Ti strongly favor a $J^\pi=3^+$ attribution. The measured Q_β values for the ^{52}Ca (5.7 ± 0.2 MeV) and ^{52}Sc (8.02 ± 0.25 MeV) decay are noticeably lower than expected from mass systematics. The energy level diagrams of ^{52}Ca, ^{52}Sc, and ^{52}Ti nuclei have been calculated in the framework of the shell model with a realistic interaction. Good agreement between theory and experiment is achieved as well for excitation energies as for mass excesses, assuring then the applicability of the theory to this region of nuclei far from stability.

I. INTRODUCTION

An extension of the known experimental properties of neutron-rich nuclei up to $N=32$ in the vicinity of the doubly closed nuclide ^{48}Ca is of fundamental interest in providing a test for shell model calculations very far from stability. The observation of ^{52,53}Sc produced in damped collisions of 8.3 MeV/nucleon ^{56}Fe ions with ^{238}U was previously reported by Breuer *et al.*[1] but no information on the decay properties could be obtained. Recently, the very high yield of alkali elements from on-line isotope separation was used to identify very neutron-rich K and Ca isotopes produced in the fragmentation of Ir by 10 GeV protons of the CERN Synchrotron.[2] Using a high efficiency neutron detector, half-lives have been determined for $^{50-54}$K and ^{53}Ca, and delayed neutron emission probabilities have been measured for $^{49-53}$K.

In this paper, we report on a study of the decay of ^{52}K, ^{52}Ca, and ^{52}Sc nuclei produced by the fragmentation of a U target with the 600 MeV proton beam of the CERN synchrocyclotron. The data obtained on these nuclei are then compared to the results of shell model calculations in the framework of a systematic study of neutron-rich nuclei in the *fp* shells. These results supersede those obtained in a preliminary measurement performed during the first yield tests and reported previously.[3]

II. EXPERIMENTAL PROCEDURE

The very neutron-rich isotopes of the light elements at ISOLDE are produced by bombarding ~13 g/cm^2 uranium carbide targets or more recently by bombarding a 122 g/cm^2 tantalum foil target with the 2.5 μA proton beam of the CERN 600 MeV synchrocyclotron. The complex mixture of radioactive nuclei was extracted from the target material and transported to an ion source via high temperature (2200° C) diffusion and desorption processes. The Ca and K isotopes were ionized with a high degree of selectivity by means of a tungsten surface ionization source. After acceleration the ion beam is subsequently mass separated in the ISOLDE facility. The beam of mass 52 was directed through a 25 m external beam line to the detector setup. Preliminary measurements with beta and neutron counters have allowed us to identify a short activity ($T_{1/2}=110\pm30$ ms) which was related to the decay of ^{52}K. A daughter β activity with $T_{1/2}\simeq5$ s was also observed and attributed to ^{52}Ca. The study of light delayed neutron emitters requires one to measure neutron spectra up to 5 MeV and to discriminate between the different final states populated by neutron emission. Two large area (2880 cm^2) plastic detectors were set up for neutron spectrometry. Each device consists of an NE110 scintillator sheet (160 cm long) bent in a radius of

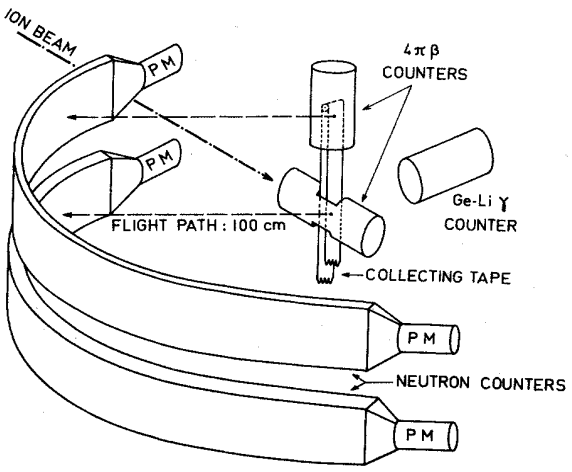

FIG. 1. Neutron time of flight setup.

curvature equal to the flight path (100 cm) and associated to two phototubes and a meantimer yielding a time resolution of 1.1 ns. The two neutron counters were identical except for thickness, 1.25 and 5.0 cm, and thereby had a detection efficiency of 9% and 36%, respectively, for 2 MeV neutrons with a proton detection threshold of 0.7 MeV. Their timing properties combined with the large solid angle (290 msr) of the detectors allow for coincidence measurements with a Ge(Li) γ counter. A schematic view of the neutron detection device is shown in Fig. 1. The mass separated ion beam is collected on the Mylar tape of the transport system inside a cylindrical beta detector which gives the start of the time of flight measurement. The short-lived isotope of the radioactive chain being detected at the collection point, a subsequent measurement of the daughter activity can be performed by moving the tape to the second detection station located 20 cm above. This layout was used to search simultaneously for ^{52}K and ^{52}Ca neutron emission. For γ measurements, two Ge(Li) detectors (13% and 20% efficiency) could be placed at these lower or upper detection stations and used either in a multianalysis mode (2×4096 channels) or in a $2048\times2048\times1024$ configuration for γ-γ-t measurements.

For total β decay energy measurements, the upper detection station was modified in order to perform β-γ measurements with a Ge(Li) counter and a β telescope. The latter consists of a 0.5 mm scintillator sheet as an energy loss detector for γ ray rejection and a 110 mm diameter, 120 mm long plastic NE102 counter for energy analysis. Biparametric β-γ events (2048×4096) were registered on magnetic tape. The electron spectrum with a selected γ ray is obtained by software gating of the coincidence data, and the corresponding background spectrum resulting from an "off peak" gate is subtracted. As the counting rate in both detectors is rather low, random coincidences are negligible. On-line calibration of the β telescope was achieved by means of ^{26}Na and ^{46}K sources produced by the ISOLDE separator, providing references at $E_\beta = 7517\pm23$, 6371 ± 16, and 2668 ± 16 keV. Endpoint energies were calculated by appropriately weighted least squares fit of the Fermi-Kurie plot of the data. The Fermi-Kurie plot of the ^{26}Na spectrum in coincidence with the 1809 keV line in the daughter is shown in Fig. 2, as an example of the weighted linear least squares fit obtained.

III. RESULTS

A. K and Ca beam intensities

The intensities of the K and Ca beams are strongly dependent on target material, rest gas pressure, and tem-

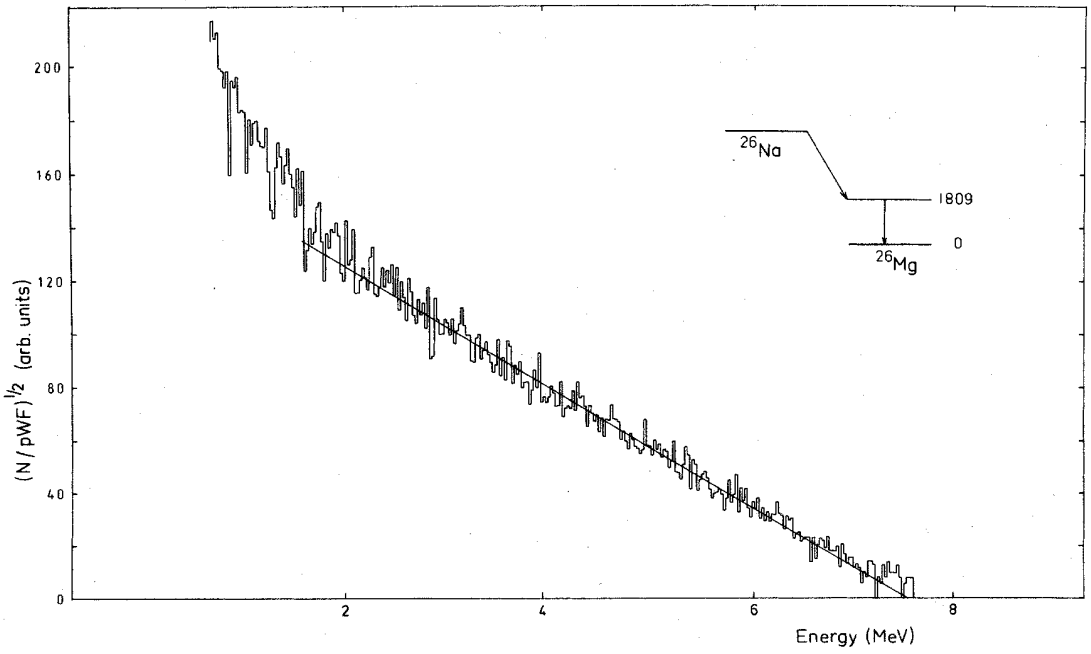

FIG. 2. Fermi-Kurie plot of ^{26}Na β spectrum in coincidence with the 1809 keV line in the daughter nucleus.

TABLE I. Typical yields achieved with the ISOLDE facility.

Nucleus	Mass	Yield (atoms $s^{-1}\mu A^{-1}$) UC target 13 g/cm^2	Tantalum target 122 g/cm^2
K	37	5.0×10^2	
	38	4.5×10^4	1.5×10^4
	42	1.6×10^7	5.0×10^7
	43	2.4×10^7	5.0×10^7
	44	1.7×10^7	3.0×10^7
	45	2.0×10^7	2.3×10^7
	46	8.9×10^6	5.0×10^6
	47	2.8×10^6	8.0×10^5
	48	5.0×10^5	1.0×10^5
	49	2.4×10^4	
	50	1.6×10^3	
	51	3.1×10^2	
	52	6.5×10^0	
Ca	49	2.5×10^5	8.0×10^5
	50	2.4×10^4	2.5×10^5
	51		1.0×10^4
	52	1.0×10^2	
Sc	52	1.3×10^1	
Ti	52	1.1×10^2	
V	52	1.7×10^3	

perature. The more volatile element K is known to be released rapidly and efficiently from the used UC and Ta target materials. Since its low ionization potential ensures unity probability of ionization, the yields of the longer-lived nuclei shown in Table I essentially correspond to what was produced in the target. The lower cross section for formation of K from Ta is compensated for by the larger Ta target thickness so that the intensity of the K beams from the two targets becomes roughly equal, as seen in Table I.

The situation is somewhat different for the much less volatile element Ca. The release of this element from the two targets is less efficient since it forms refractory carbide and oxide. By increasing the ion source temperature in order to reduce the delay time losses of the short-lived K nuclei, it was observed that the originally pure beam becomes contaminated by directly ionized Ca. The intensities of the observed Ca beams are also shown in Table I. In fact, the Ca ionization potential of 6.1 eV allows a maximum of 30% surface ionization efficiency in our source. By comparison with the 100% K yield and taking into account the cross-section differences, the Ca yield can be estimated to be 28% from the Ta target and only 5% from the UC target. The lower yield from the latter target is due to the formation of CaC_2, whereas any loss of Ca as CaO in the Ta target disappears with time due to outgassing. It is interesting to note that primary ionized beams of the elements Sc, Ti, and V were observed for the first time with intensities shown in Table I.

B. ^{52}K decay

Using usual mass formulae,[4,5] the decay energy $^{52}K\rightarrow{}^{52}Ca$ and the neutron separation energy in ^{52}Ca can be evaluated, respectively, as $Q_\beta=16$ MeV and $S_n=5.8$ MeV. The delayed neutron emission is therefore expected to be the main decay mode for ^{52}K. The half-life has been measured by multiscaling the beta emission detected at the collection station, and was found to be $T_{1/2}=110\pm30$ ms. This value is consistent with a more precise value measured in a recent experiment[2] by β-coincident neutron counting ($T_{1/2}=105\pm5$ ms). The neutron spectrum was

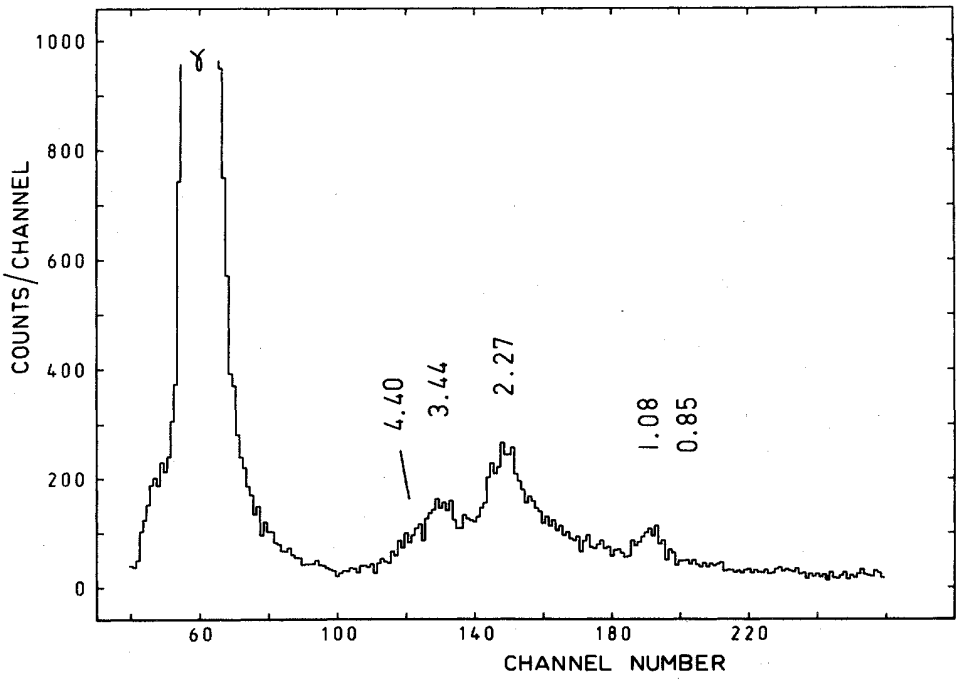

FIG. 3. Delayed neutron spectrum in the ^{52}K decay.

TABLE II. Neutron energies, excitation energies, β branching, and logft values in ^{52}K decay.

E_n (MeV)	Final state in ^{52}Ca (MeV)	I_β (%)	logft
4.40±0.08	10.29	14.5±1.7	4.0±0.1
3.44±0.06	9.31	23.3±1.8	4.1±0.1
2.27±0.04	8.11	41.9±2.4	4.2±0.1
1.08±0.02	6.90	17.1±1.0	4.9±0.1
0.85±0.02	6.67	3.2±0.3	5.7±0.1
	2.56	<20	>5.5

measured with the more efficient curved scintillator (Fig. 1) designed for very low yields (50—70 atoms/s in this case). The time of flight spectrum of the delayed neutrons is shown in Fig. 3. This spectrum was unfolded for detector response and corrected for efficiency. The energy and intensity of neutrons assigned to the decay of ^{52}K are listed in Table II.

A separate experiment was performed to search for electromagnetic transitions in the decay of ^{52}K. A first investigation was undertaken in which the species were collected during 400 ms, their β coincident γ activity multianalyzed (2×200 ms) and removed for background reduction. Evidence for prompt γ lines was not clear, indicating that, in addition to the low yield, the branching ratio for bound states is weak. In order to improve the statistical quality of the data, the γ measurement was then carried out during a 4 s collection [Fig. 4(a)] and, in a separate spectrum, during the subsequent 4 s decay time [Fig. 4(b)]. Following this procedure during 2340 cycles one single line ($E_\gamma=2563\pm1$ keV) is clearly observed in the first spectrum only, as expected in the case of a $T_{1/2}=110$ ms emitter. Except for the 2563 keV line which is attributed to the ^{52}K decay, all peaks have been identified and belong to the decay of ^{52}Ca ^{52}Sc, ^{52}Ti, or ^{52}V. The region around 2.5 MeV of the two spectra is shown in Fig. 4. The 2563 keV transition is suggested to be the $2^+\rightarrow0^+$ in ^{52}Ca as it appears the most plausible explanation for the presence of this line in our spectrum for the following reasons:

This line is the only γ line observed in the ^{52}K decay.

The beta feeding of the ^{52}Ca 2^+ state is expected to involve a parity change but is favored by the beta transition energy ($E_\beta\simeq13.4$ MeV).

The transition could take place from an excited state in ^{51}Ca populated by delayed neutrons. It would imply the beta feeding of a state in ^{52}Ca with $E_\gamma>8.4$ MeV and $E_\beta<7.6$ MeV. From our previous measurements of ^{51}K$\rightarrow$^{51}Ca decay,[6] no state at $E_x=2.56$ MeV has been observed in ^{51}Ca.

The level scheme of ^{52}Ca established on the basis of our neutron and γ measurements is shown in Fig. 5. The intensity of the β transition to the ground state of ^{52}Ca was not measured and is assumed to be negligible. This as-

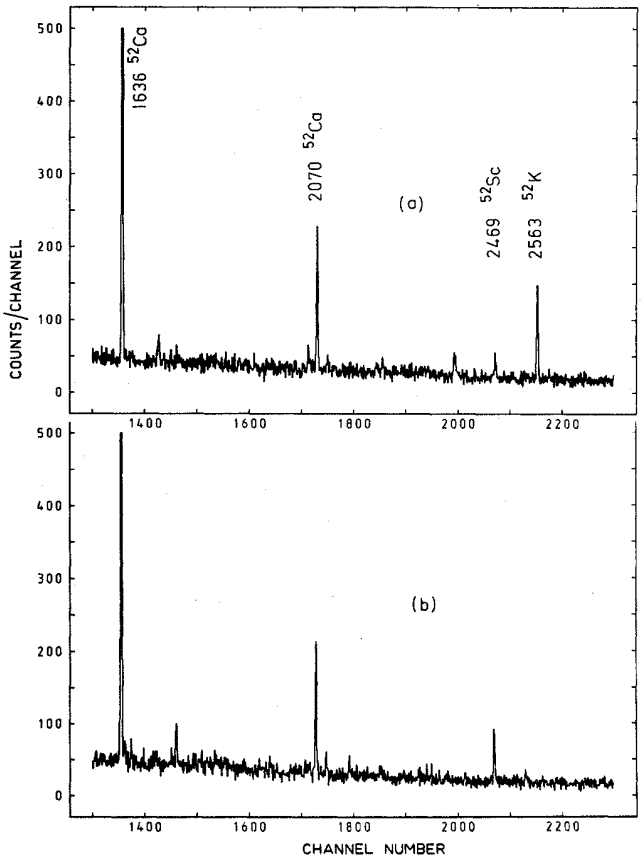

FIG. 4. The 1.6 to 2.8 MeV region of the γ spectra registered from ^{52}K sources, (a) during the collection, (b) during the decay.

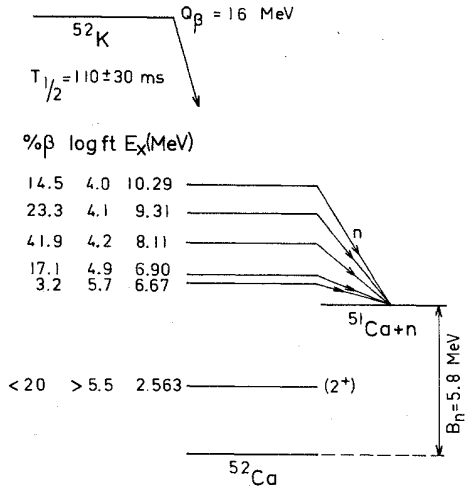

FIG. 5. Decay scheme of ^{52}K.

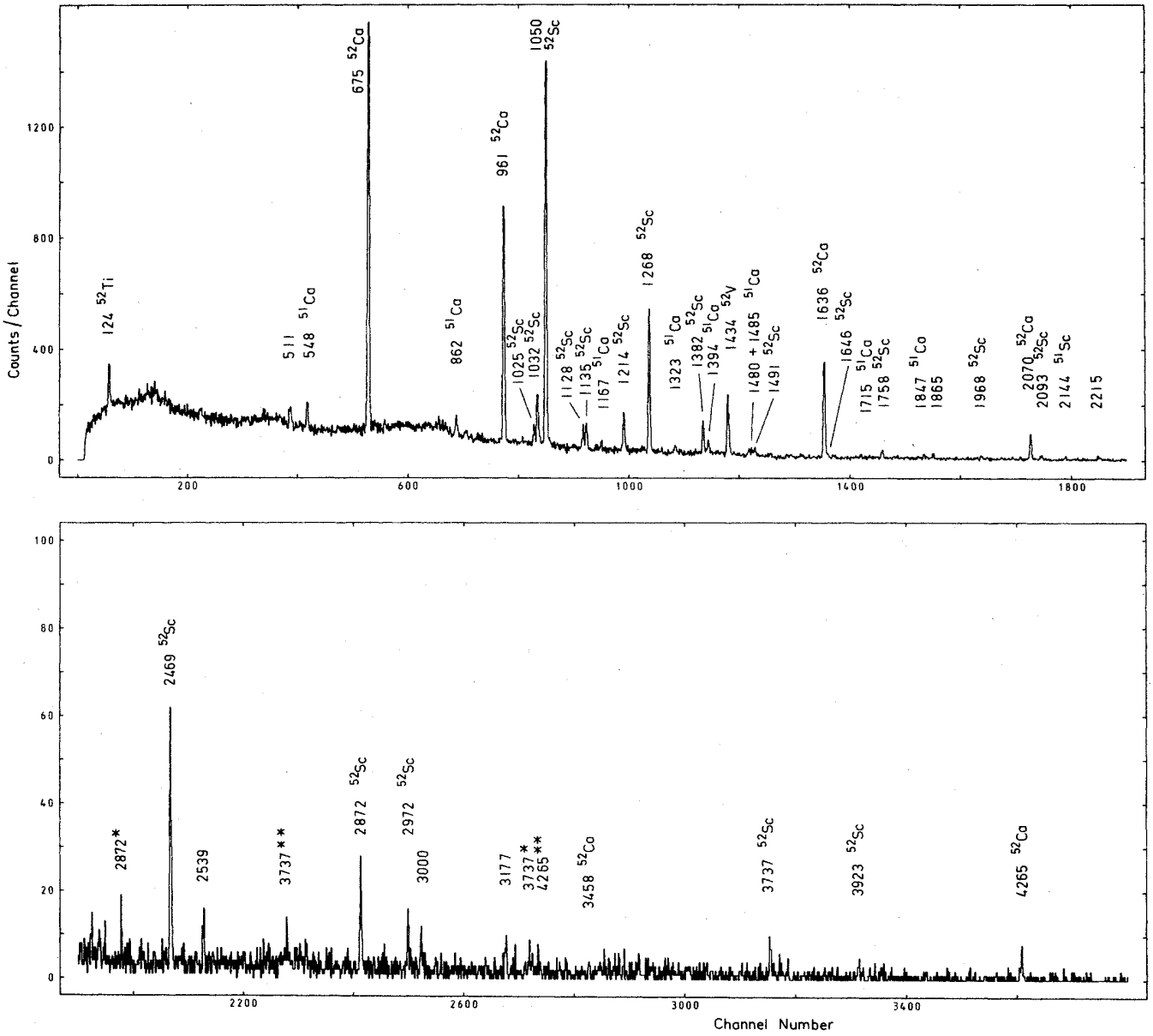

FIG. 6. β-coincident γ spectrum subsequent to the ^{52}Ca decay.

sumption is valid only in the case of a second forbidden transition. It has not been possible to obtain a reliable value for the beta branching ratio to the bound state at 2.56 MeV, as direct production of calcium ions took place in the ion source and prevented a P_n determination from the γ spectra. Therefore only a limit is indicated for this transition which is consistent with the P_n value measured with a different setup[2] ($P_n = 108 \pm 20$). It must be noted that ^{52}K is a possible two neutron emitter ($Q_\beta - S_{2n} \simeq 7$ MeV), but no evidence for ^{50}Ca decay was found in the γ spectra.

C. ^{52}Ca→^{52}Sc

The decay of ^{52}Ca and ^{52}Sc was studied in the same experiment, these nuclei being obtained as daughter activity of ^{52}K or resulting from calcium and scandium ions, produced by the source according to the operating conditions. Using an 8 s cycle (collection time equal to measuring time), sources were transported to the detection station located above the collection point (Fig. 1).

Attribution of all transitions to the relevant decays is based on the measurements which were carried out for a total number of cycles equal to 14 000:

(a) β-coincident γ multianalysis (2×4 s);

(b) γ-γ-t coincidence measurement.

Figure 6 shows the energy spectrum of the β-coincident γ activities, recorded during two successive periods of 4 s. Using weighted mean values from the decay rate of the prominent peaks in the multispectrum, two new activities were observed.

TABLE III. Energy and relative intensity of transitions in ^{52}Sc following β decay of ^{52}Ca.

E_γ (keV)	I_γ[a]	E_i (MeV)	E_f (MeV)
675.2±0.3	100	0.68	0
961.2±0.3	80	1.64	0.68
1636.4±0.2	57	1.64	0
2070.4±0.6	18	2.75	0.68
3458.0±1.0	1.0	3.46	0
4265.5±1.5	2.2	4.27	0

[a]For absolute intensity per 100 decays multiply by 0.62.

An 8.2±0.2 s half-life is inferred from the decay rate of lines at 1050, 1214, 1268, and 1382 keV. These energies correspond to transitions in ^{52}Ti and allow us to assign the 8.2 s activity to the decay of ^{52}Sc.

A 4.6±0.3 s half-life is observed in the decay of other lines (e.g., 675, 961, 1636, and 2070 keV) and is attributed to the activity of the ^{52}Ca parent. This assignment was confirmed by the results of separate multispectrum measurements where the decay of ^{52}K ($T_{1/2}=110$ ms) and the growth of ^{52}Ca ($T_{1/2}=4.6$ s) were simultaneously observed.

The energy and intensity of γ rays assigned to the decay of ^{52}Ca are listed in Table III. Branching ratios in ^{52}Sc deduced from this experiment are reported in Table IV. Precise excitation energies in ^{52}Sc, β branching, and logft values in ^{52}Ca decay are given in Table V. The logft values were deduced from the Gove and Martin logft tables,[7] together with the values $T_{1/2}=4.6$ s and $Q_\beta=5.7\pm0.2$ MeV determined in the present experiment (see below).

The logft values were used in association with the rules of Raman and Gove[8] to deduce the $J^\pi=1^+$ assignment proposed for the levels at 1.64, 2.75, 3.46, and 4.27 MeV. The intensity of the β transition to the ground state of ^{52}Sc was not measured and was assumed to be negligible, since the ^{52}Sc ground state is expected to be a member of the $J^\pi=(2-5)^+$ multiplet resulting from the $1f_{7/2}\times2p_{3/2}$ coupling (see the following section), an assumption which is in agreement with the decay scheme ^{52}Sc→^{52}Ti investigated in this work. In Fig. 7, the level scheme of ^{52}Sc summarizes the first information on electromagnetic transitions in ^{52}Sc.

As ^{52}Ca is a possible delayed neutron emitter (for ^{52}Sc, $S_n=4.89$ MeV), the existence of neutron activity was searched for with the 1.25 cm thick neutron spectrometer located at the upper detection station and operated during the γ measurement. No neutron emission has been observed.

TABLE IV. γ-ray branching ratios in ^{52}Sc.

E_i (MeV)	E_f (MeV)	Branching ratio (%)
0.68	0	100
1.64	0	42±2
	0.68	58±2
2.75	0.68	100
3.46	0	100
4.27	0	100

TABLE V. Excitation energies, β branching, and logft values in ^{52}Ca decay.

Final state in ^{52}Sc (keV)	I_β (%)	logft[a]
675.2±0.3	<5	>5.9
1636.4±0.2	86.8±1.3	4.2±0.1
2745.6±0.7	11.2±1.2	4.5±0.2
3458.1±1.0	0.6±0.3	5.3±0.5
4265.7±1.5	1.4±0.4	4.0±0.5

[a]The quoted uncertainties are derived from the errors on the half-life, the I_β values, and the ±200 keV contribution from the Q_β value.

The Q_β value of the ^{52}Ca→^{52}Sc has been measured from the electron spectra in coincidence with the 961 and 1636 keV γ lines, summed up, and gives a resulting spectrum of 4500 counts. As can be seen from the decay scheme, the obtained spectrum corresponds only to the β feeding of the 1636 keV level and there is no contribution from higher located levels. The Fermi-Kurie plot analysis of the data (Fig. 8) yields a β endpoint energy of $E_\beta=4055\pm200$ keV. The quoted error is large compared to the one calculated according to the formula developed by Rehfield[9] but takes into account the fact that the endpoint position depends on the region of the Fermi-Kurie plot over which the least squares fit is operated. The resulting Q_β value (5.7±0.2 MeV) of the ^{52}Ca→^{52}Sc decay differs appreciably from the various theoretical estimates reported up to now (Table VI).

D. ^{52}Sc→^{52}Ti

Previous studies of the $T_z=4$ nucleus ^{52}Ti have been performed either by the two neutron transfer reaction

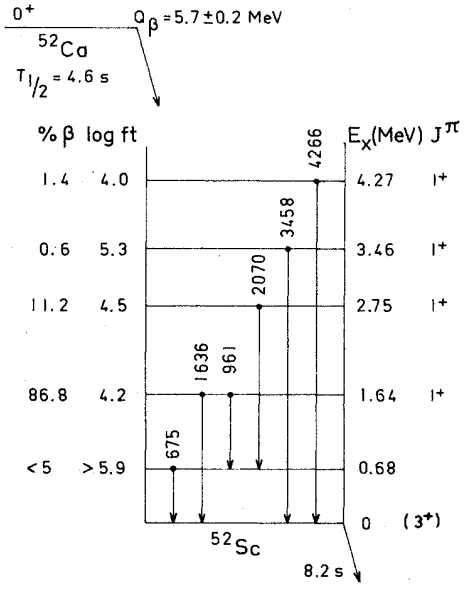

FIG. 7. Decay scheme of ^{52}Ca.

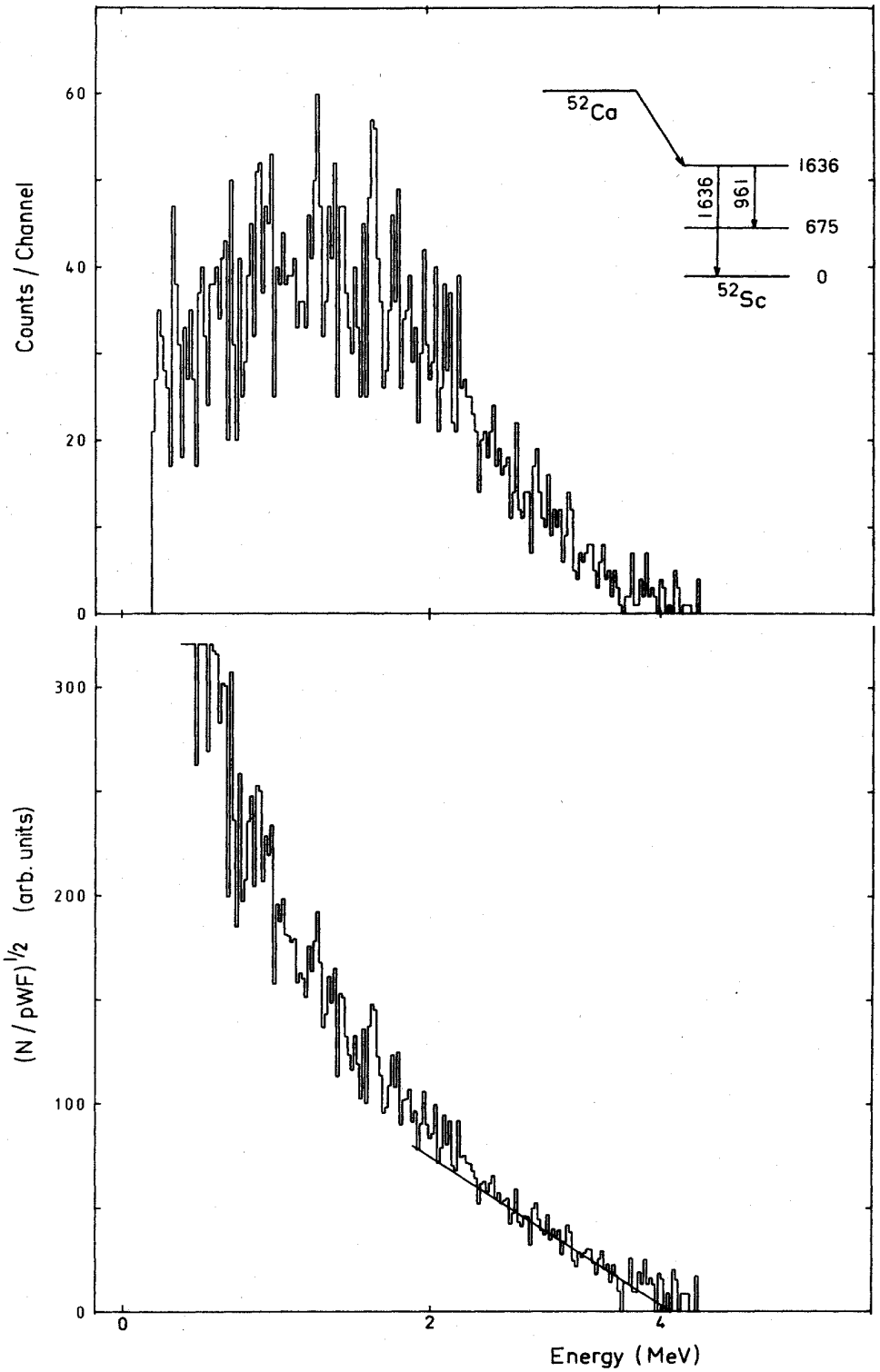

FIG. 8. Spectrum of the β branch to the 1.64 MeV level in ^{52}Sc and the corresponding Kurie plot.

^{50}Ti(t,pγ) (Ref. 10) or by the heavy-ion-induced reaction and high spin yrast states observation [^{48}Ca(^{7}Li,p2nγ) (Ref. 11)]. These reactions selectively populate the low energy states of ^{52}Ti, giving, in particular, information on states belonging to the $(\pi f_{7/2})^2(\nu p_{3/2})^2$ configuration. The beta decay of ^{52}Sc populates states which are weakly excited in these reactions. From the analysis of γ-γ and γ-multispectrum measurements we have built a decay scheme (Fig. 9) which accounts for 13 excited levels in ^{52}Ti, only four of which were reported in the previous

TABLE VI. Comparison between the experimental Q_β value and semiempirical estimates in the decay of ^{52}Ca.

	$Q_\beta(^{52}\text{Ca}\text{-}^{52}\text{Sc})$ (MeV)
Measured value (this experiment)	5.7±0.2
Semiempirical predicted values[a]	
Myers	7.75
Groote *et al.*	7.14
Seeger and Howard	7.5
Liran and Zeldes	7.06
Jänecke *et al.*	6.94
Comay and Kelson	6.87
Möller and Nix[b]	7.78

[a]Reference 4 unless otherwise quoted.
[b]Reference 5.

studies. Energy and relative intensity of transitions in ^{52}Ti following β decay of ^{52}Sc are listed in Table VII. For the few transitions where comparison with existing data can be made, results are found consistent but more precise. γ ray branching ratios in ^{52}Ti are given in Table VIII. Beta branching and logft values in the ^{52}Sc decay (Table IX) were calculated with the use of $T_{1/2}=8.2$ s and $Q_\beta=8.02$ MeV, measured in the present experiment. The intensity of the β transitions to the 2^+ state in ^{52}Ti ($E=1.05$ MeV) and to the (4^+) state ($E=2.32$ MeV) suggests $J=3$ for the angular momentum of the ^{52}Sc ground state.

For the ^{52}Sc→^{52}Ti disintegration, two independent determinations of the Q_β value were performed. The high energy region of the electron spectrum obtained in coincidence with the 1050 keV γ line corresponds to the β feeding of the 1.05 MeV level. Since 75% of the β decay strength feeds upper levels in ^{52}Ti, the energy range for the least squares fit in the Fermi-Kurie plot is restricted to the highest 1 MeV of the data. The least squares fit of the Fermi-Kurie plot of the data in the region of interest yields an endpoint of $E_\beta=7044\pm165$ keV (Fig. 10), very close to the calibration point provided by ^{26}Na ($E_\beta=7517$ keV). The corresponding Q_β value is 8094±165 keV.

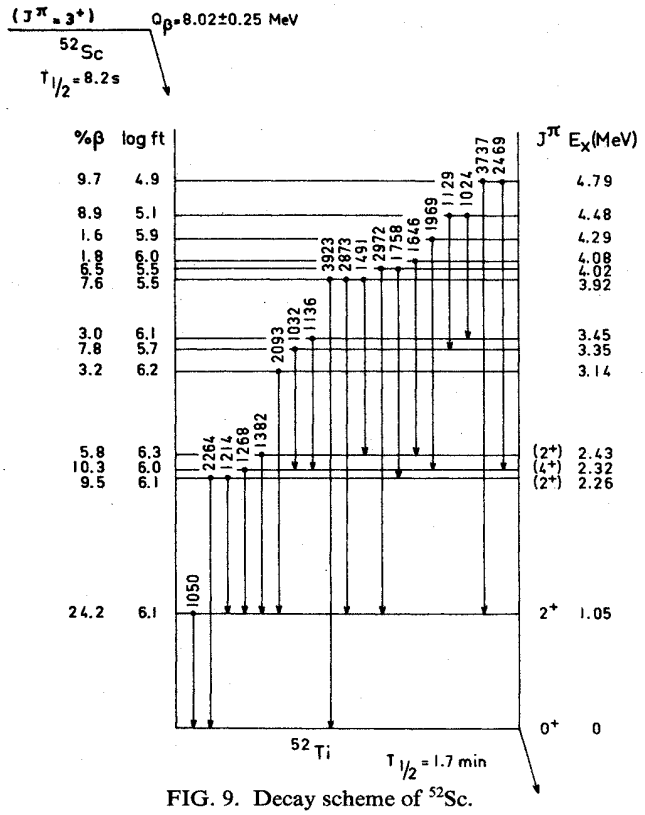

FIG. 9. Decay scheme of ^{52}Sc.

TABLE VII. Energy and relative intensity of transitions in ^{52}Ti following β decay of ^{52}Sc.

E_γ (keV)	I_γ[a]	E_i (MeV)	E_f (MeV)
1025.0±0.5	3.5±0.7	4.48	3.45
1032.3±0.3	14±1	3.35	2.32
1049.7±0.1	100	1.05	0
1128.1±0.3	5.5±0.8	4.48	3.35
1135.0±0.3	7±1	3.45	1.05
1214.5±0.3	12±1	2.26	1.05
1267.9±0.1	40±3	2.32	1.05
1381.9±0.2	11±1	2.43	1.05
1491.0±0.5	3.0±0.6	3.92	2.43
1646.0±0.6	1.9±0.6	4.08	2.43
1758.2±0.3	4.1±0.7	4.02	2.26
1968.4±0.9	1.7±0.5	4.29	2.32
2093.4±0.7	3.3±0.6	3.14	1.05
2265.2±1.3	1.6±0.4	2.26	0
2468.8±0.4	8±1	4.79	2.32
2872.0±0.5	3.9±0.7	3.92	1.05
2972.2±0.5	2.6±0.5	4.02	1.05
3737.2±1.1	2.1±0.5	4.79	1.05
3923.0±2.8	0.9±0.3	3.92	0

[a]For absolute intensity per 100 decays multiply by 0.976.

TABLE VIII. γ-ray branching ratios in ^{52}Ti.

E_i (MeV)	E_f (MeV)	Branching ratio (%)
1.05	0	100
2.26	0	11±3
	1.05	89±3
2.32	1.05	100
2.43	1.05	100
3.14	1.05	100
3.35	2.32	100
3.45	2.32	100
3.92	0	11±4
	1.05	50±6
	2.43	39±6
4.02	1.05	38±6
	2.26	62±6
4.08	2.43	100
4.29	2.32	100
4.48	3.35	61±6
	3.45	39±6
4.79	1.05	21±4
	2.32	79±4

The second estimate was obtained from the β spectrum in coincidence with the 1032 keV γ line, for which a β endpoint of $E_\beta=4594\pm160$ keV was found, yielding a Q_β value of 7944±160 keV. The errors calculated from the Rehfield formula are rather large due to poor statistics. It is noteworthy that the energy difference between the two E_β endpoints ($\Delta E_\beta=2.45$ MeV) is in agreement, within the errors, with the energy separation of the 3.35 and 1.05 MeV levels. The Q_β value resulting from these measurements is 8.02±0.25 MeV, which is again significantly lower than the up to now published theoretical estimates. A comparison between semiempirical mass evaluations and the experimental result is presented in Table X.

IV. SHELL MODEL CALCULATIONS

Previous theoretical work in this region[12] of *fp* shell nuclei has led to a description of all the $1f_{7/2}$ nuclei using the standard shell model approach with realistic interactions with well-behaved monopole terms. The nuclei considered in this paper provide the natural extension of that work and are a test of the validity of the model and interaction far from stability. The valence space adapted to these nuclei includes the orbits $1f_{7/2}$, $2p_{3/2}$, $1f_{5/2}$, and $2p_{1/2}$. The lowest energy configurations are $(1f_{7/2})^8r^4$ (r means the three other orbits) for the ^{52}Ca ground state, and $(1f_{7/2})^9r^3$ for the 1^+ states in ^{52}Sc. In spite of the large isospins involved, the dimensions of the basis grow rapidly when including more configurations; therefore, we shall limit ourselves to 1p-1h jumps from $1f_{7/2}$ to r orbits. These kinds of excitations have proven to be crucial to have a good description of nuclei in the lower part of the *fp* shell.[13] The interaction we use is that of Ref. 13, which consists of the Kuo-Brown interaction with a few monopole changes, and it is called KB3 in the above-mentioned reference.

TABLE IX. Excitation energies, β branching, and logft values in the ^{52}Sc decay.

Final state ^{52}Ti (keV)	I_β (%)	logft
1049.7±0.1	24.2±5.7	6.1±0.2
2264.7±0.3	9.5±1.6	6.1±0.2
2317.6±0.1	10.3±3.3	6.1±0.2
2431.6±0.2	5.8±1.4	6.3±0.2
3143.1±0.7	3.2±0.7	6.3±0.2
3349.9±0.3	7.8±1.6	5.8±0.2
3452.6±0.3	3.0±1.2	6.2±0.3
3922.1±0.7	7.6±1.1	5.6±0.2
4022.2±0.5	6.5±1.0	5.6±0.2
4077.6±0.7	1.8±0.6	6.1±0.3
4286.0±1.0	1.6±0.5	6.1±0.3
4477.9±0.7	8.9±1.2	5.2±0.2
4786.5±0.6	9.7±1.3	5.0±0.2

TABLE X. Comparison between the experimental Q_β value and semiempirical estimates in the decay of ^{52}Sc.

	Q_β(^{52}Sc-^{52}Ti) (MeV)
Measured value (this experiment)	8.02±0.25
Semiempirical predicted values[a]	
Myers	11.1
Groote *et al.*	9.96
Seeger and Howard	11.3
Liran and Zeldes	9.94
Jänecke *et al.*	9.95
Comay and Kelson	9.92
Möller and Nix[b]	11.24

[a]Reference 4 unless otherwise quoted.
[b]Reference 5.

A. A previous step: the ^{50}Sc

This nucleus is the anti-Pandya transform of the ^{52}Sc. Calculations in it have much smaller dimensions and compare with better known experimental data. We perform this calculation, which will serve as a guide, and present the results in Fig. 11. First notice the result of column KB3 (f^9r) where we have not included 1p-1h excitations. While the ground state multiplet (essentially $1f_{7/2}^9 2p_{3/2}$ states) is nicely reproduced, 1^+ states lie at least 1 MeV higher in energy than experimentally. Coming to column KB3 ($f^9r+f^8r^2$), we see that the main effect of enlarging the space is to lower the 1^+ states. Nevertheless, the density of 1^+ states in the calculation, up to 5 MeV, is still smaller than in the experiment. A similar situation is found in ^{48}Sc. The gain in energy of the ground state multiplet by increasing the space is very small (0.65 MeV, dimensions going from 2 to 63).

B. The parent nucleus ^{52}Ca

The experimental information is very limited: the ground state (0^+) half-life ($t_{1/2}=4.6\pm0.3$ s), and the energy of the first excited level (2^+, 2.56 MeV).

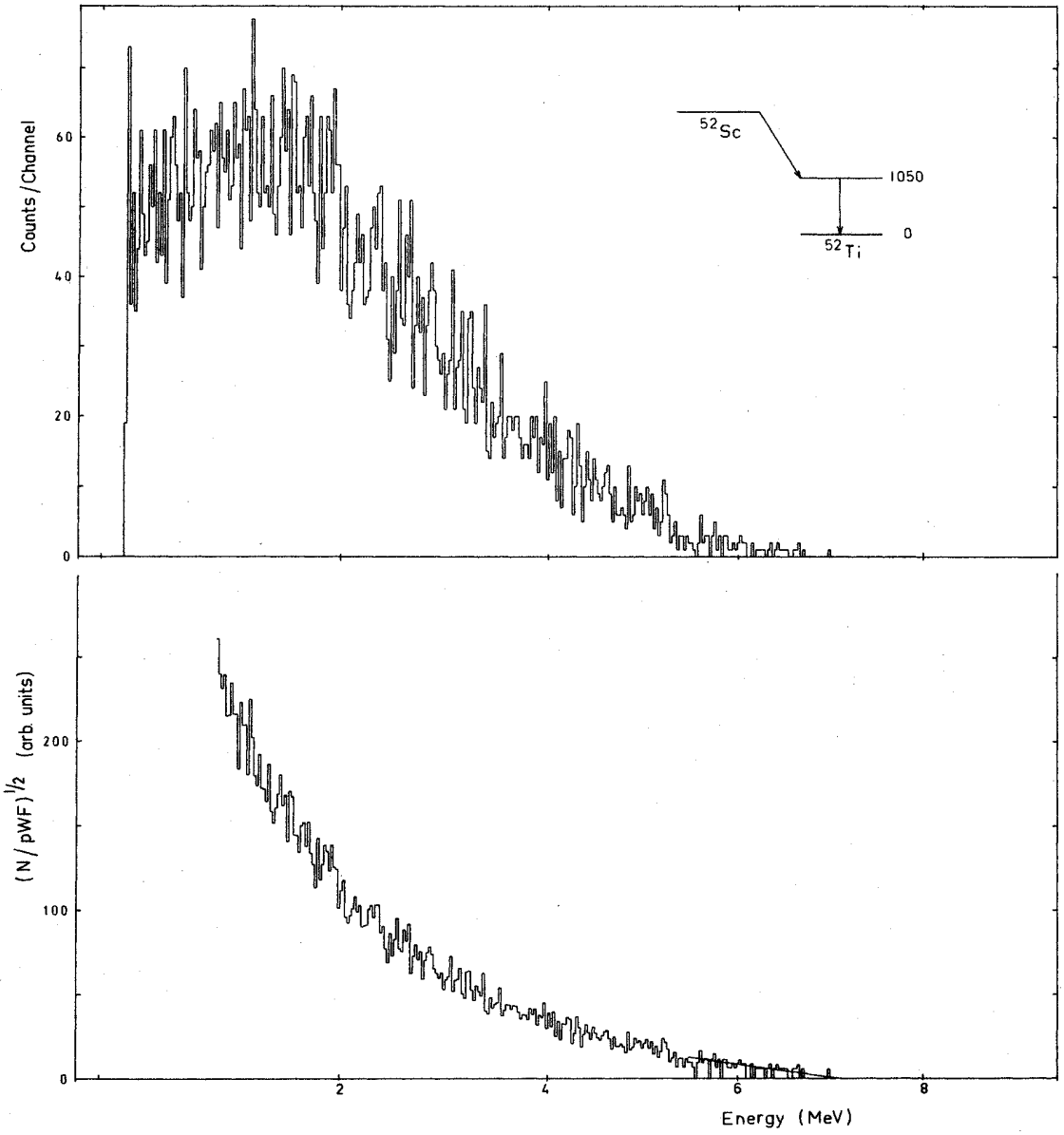

FIG. 10. Spectrum of the β rays in coincidence with the 1050 keV γ line in ^{52}Ti and the corresponding Kurie plot.

The calculation including the f^8r^4 and f^7r^5 configurations gives a ^{52}Ca nuclear binding energy relative to ^{40}Ca of -97.34 MeV, and an excitation energy of the first 2^+ state of 2.28 MeV. The ground state wave function obtained is

$$|0^+T=6\rangle = 0.94\,|f^8_{7/2}p^4_{3/2}\rangle + 0.29\,|f^8_{7/2}p^2_{3/2}p^2_{1/2}\rangle + 0.10\,|f^8_{7/2}p^2_{3/2}f^2_{5/2}\rangle + \cdots .$$

Its knowledge could allow us to obtain a qualitative insight into the Gamow-Teller (GT) transition probabilities to 1^+ states in ^{52}Sc.

The excitation energy of the first 2^+ in ^{52}Ca is plotted in Fig. 12 together with the 2^+ systematics in even calcium isotopes. The figure is suggestive of the semimagic character of the nucleus ^{52}Ca due to the closure of the $2p_{3/2}$ subshell.

C. The ^{52}Sc level scheme

The calculation of the ^{52}Sc ground state multiplet in the model space $(f^9r^3+f^8r^4)$ is far beyond our computing possibilities (dimensions >500). We perform a f^9r^3 calculation whose results are shown in Fig. 13.

(i) The ground state multiplet agrees quite well with the available data. We predict a 3^+ ground state compatible with the experimental indication.

(ii) In that model space there are five low lying 1^+ states with the structures $f^9_{7/2}p^2_{3/2}f_{5/2}$ (four states) and $f^9_{7/2}p^2_{3/2}p_{1/2}$ (one state). Comparing with the experimen-

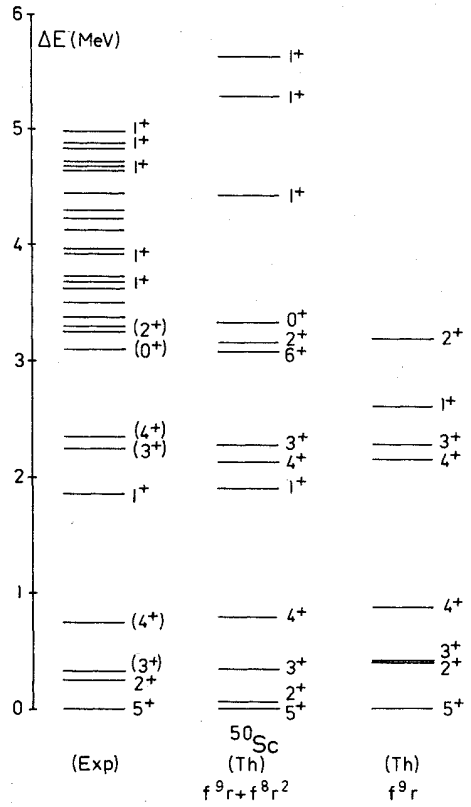

FIG. 11. Calculated and experimental level diagrams of ^{50}Sc.

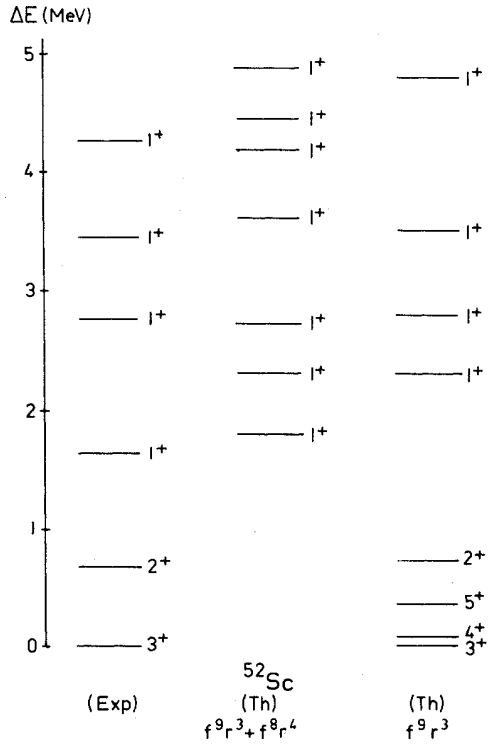

FIG. 13. Calculated and experimental level diagrams of ^{52}Sc.

tal level scheme we notice that all the 1^+ states lie high in excitation energy, as was the case in the ^{50}Sc calculation. The level density seems to be correct; nevertheless as the second 1^+ state has a $f^9_{7/2}p^2_{3/2}p_{1/2}$ dominant structure and cannot be fed by a GT transition from the ^{52}Ca ground state, the actual agreement is worse.

To improve the theoretical description, we shall use the results of the ^{50}Sc calculation, where we have seen that (i) the inclusion of f^8r^2 configurations does not change the results for the ground state multiplet and (ii) the low lying 1^+ states have a net gain of (0.6 ± 0.1) MeV relative to the ground state upon inclusion of those configurations. We assume the same behavior in the ^{52}Sc case, and proceed to calculate only the 1^+ states in the $(f^9r^3+f^8r^4)$ space. Once this is done, we locate the first one at an excitation energy 0.6 MeV lower than in the f^9r^3 calculation and the other 1^+'s follow. The results are presented in Fig. 14. There we can see we have done much better; the calculated levels are in one to one correspondence with the experimental ones, except in the 1^+_2(calc), and this for the reasons quoted above. The agreement can be qualified as very good. The dominant component of the five lower 1^+ states happens to be the same as in the f^9r^3 calculation. From the analysis of the wave functions we conclude that the GT β decay proceeds through small components of the wave function of the parent state, precluding any sim-

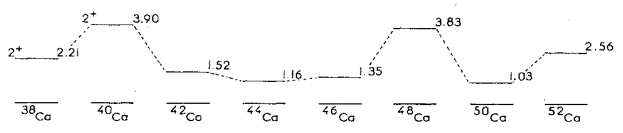

FIG. 12. 2^+ systematics in the even calcium nuclei.

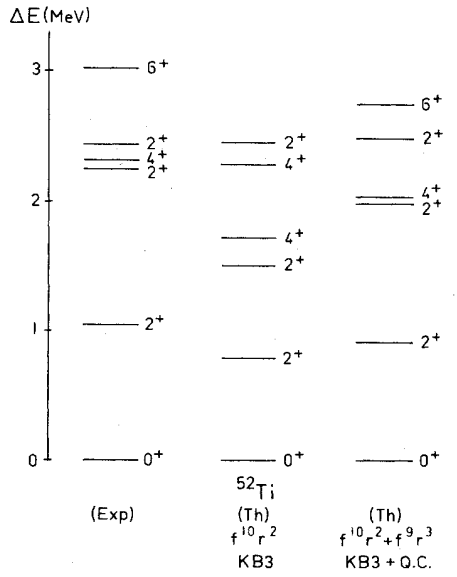

FIG. 14. Calculated and experimental level diagrams of ^{52}Ti.

ple estimate of the logft values of the different transitions.

D. ^{52}Ti and Q_β values

The same approach has been used for the last nucleus of the series, ^{52}Ti. In Fig. 13 we show the results of $f^{10}r^2$ and $(f^{10}r^2+f^9r^3)$ calculations. Again the level scheme gets improved when the 1p-1h jumps are included. In that case we have included the 2p-2h jumps in the interaction with the quasiconfiguration method (for this reason we write KB3 + QC in the figure). In the calcium and scandium this is not necessary because the space can cope with all the relevant pairings between the $1f_{7/2}$ and $2p_{3/2}$ shells.

Finally, from our calculations we get a consistent theoretical estimate of the relevant Q_β values. The results in the smallest spaces using a $1f_{7/2}$ single particle Coulomb energy of 7.0 MeV following Ref. 14 and a two-body Coulomb matrix element of 0.4 MeV are as follows:

$$Q_\beta(^{52}\text{Ca}\text{-}^{52}\text{Sc})=5.3 \text{ MeV} ,$$

$$Q_\beta(^{52}\text{Sc}\text{-}^{52}\text{Ti})=7.2 \text{ MeV} .$$

They have to be compared with the experimental ones:

$$Q_\beta(^{52}\text{Ca}\text{-}^{52}\text{Sc})=5.7\pm0.2 \text{ MeV} ,$$

$$Q_\beta(^{52}\text{Sc}\text{-}^{52}\text{Ti})=8.02\pm0.25 \text{ MeV} .$$

In both cases our values fall quite far from the mass formulae predictions, dramatically improving the agreement.

V. CONCLUSIONS

A detailed study of the beta decay of ^{52}K, ^{52}Ca, and ^{52}Sc has been performed using neutron, beta, and gamma spectroscopy techniques. From the decay schemes established in this work different properties of these very neutron-rich isotopes can be compared to previous results relative to lighter isotopes. The Q_β values are found to differ noticeably from mass systematics. A shell model calculation is presented which shows that the structure of the nuclei ^{52}Ca, ^{52}Sc, and ^{52}Ti is given by the dominant $f^{12-n}r^n$ ($n=4$, 3, and 2, respectively) configurations dressed by the 1p-1h jumps, $f^{11-n}r^{n+1}$. Energy levels and Q_β values agree nicely with the measured values. These results support the validity of the model space, fp-minimal + (1p-1h), far from stability. Moreover, the Kuo-Brown[15] realistic interaction, with its monopole part adjusted to reproduce the spectroscopy at the stability valley, proves to be suitable far from stability.

[1]H. Breuer, K. L. Wolf, B. G. Glagola, K. K. Kwiatkowski, A. C. Mignerey, V. E. Viola, W. W. Wilcke, W. U. Schröder, J. R. Huizenga, D. Hilscher, and J. Birkelund, Phys. Rev. C **22**, 2454 (1980).

[2]M. Langevin, C. Détraz, D. Guillemaud-Mueller, A. C. Mueller, C. Thibault, F. Touchard, G. Klotz, C. Miehé, G. Walter, M. Epherre, and C. Richard-Serre, Phys. Lett. **130B**, 251 (1983).

[3]A. Huck, G. Klotz, A. Knipper, C. Miehé, C. Richard-Serre, and G. Walter, in the Fourth International Conference on Nuclei Far From Stability, Helsingør, 1981, CERN Report 81-09, 1981, p. 378.

[4]W. D. Myers, At. Data Nucl. Data Tables **17**, 411 (1976); H. V. Groote, E. R. Hilf, and K. Takamashi, *ibid.* **17**, 418 (1976); P. A. Seeger and W. M. Howard, *ibid.* **17**, 428 (1976); S. Liran and N. Zeldes, *ibid.* **17**, 431 (1976); J. Jänecke, *ibid.* **17**, 455 (1976); E. Comay and I. Kelson, *ibid.* **17**, 463 (1976).

[5]P. Möller and J. R. Nix, At. Data Nucl. Data Tables **26**, 165 (1981).

[6]A. Huck, G. Klotz, A. Knipper, C. Miehé, C. Richard-Serre, G. Walter, and H. L. Ravn, Phys. Rev. C **22**, 2544 (1980).

[7]N. B. Gove and M. J. Martin, Nucl. Data Tables **10**, 205 (1971).

[8]S. Raman and N. B. Gove, Phys. Rev. C **7**, 1995 (1973).

[9]D. M. Rehfield, Nucl. Instrum. Methods **157**, 351 (1978).

[10]J. G. Pronko, T. T. Bardin, J. A. Becker, T. R. Fischer, R. E. McDonald, and A. R. Poletti, Phys. Rev. C **9**, 1430 (1974); **10**, 1249 (1974).

[11]H. Gögelein, Diplomarbeit, Technische Universität München, 1973 (unpublished).

[12]E. Pasquini, Ph.D. thesis, Centre de Recherches Nucléaires, Strasbourg, 1976.

[13]A. Poves and A. Zuker, Phys. Rep. **70**, 235 (1981).

[14]E. Caurier and A. Poves, Nucl. Phys. **A385**, 407 (1982).

[15]T. Kuo and G. E. Brown, Nucl. Phys. **A114**, 241 (1968).